



Behavior of Tunisian Aleppo Pine (*Pinus halepensis* Mill) wood during convective drying: Identification of the diffusion coefficient taking into account shrinkage velocity

Kamel Ben Dhib^{a,*}, Mohamed Tahar Elaieb^b, Soufien Azzouz^a, Afif Elcafsi^a.

^aLaboratoire d'énergétique et des transferts thermique et massique. Faculté des sciences de Tunis, Université de Tunis El Manar, Campus Universitaire Manar II 2092, Tunisie.

^bLaboratoire de Gestion et de Valorisation des Ressources Forestières, Institut National de Recherches en Génie Rural, Eaux et Forêts (INRGREF), Rue Hédi KARRAY BP 210 Ariana 2080 Tunisie.

Received 12 Feb 2016, Revised 31 Mar 2016, Accepted 13 Apr 2016

*Corresponding author. E-mail: bendhib.kamel@yahoo.fr (Kamel Ben Dhib), ayeb2002@yahoo.fr (Mohamed Tahar Elaieb); Tel.: +21697980632; fax: +21670860434.

Abstract

This study proposed to identify the water diffusion coefficient in Tunisian Aleppo pine (*Pinus halepensis* Mill.) wood through convective drying, and to predict the activation energy. A diffusive model was developed based on numerical resolution of both the solid phase conservation equation and the water transfer equation (diffusion/convection). It also took into consideration the contraction speed of the solid matrix due to hydrous shrinkage. The model was developed by minimizing the difference between the experimental and the estimated moisture content. The desorption isotherm was measured by the experiment and then modeled by DENT's equation. It provided precise information about the hygroscopic wood equilibrium. DENT's equation was used to represent the relationship between water activity and the equilibrium moisture content. The volumetric shrinkage curve provided information about the different types of water in the wood as well as the water content value at the fiber saturation point. Hydrous diffusivity values varied between $1,7 \cdot 10^{-11} \text{ m}^2 \text{ s}^{-1}$ and $3,4 \cdot 10^{-11} \text{ m}^2 \text{ s}^{-1}$ as a function of temperature and water content. The activation energy was 137,031 (kJ/mol). At a critical point, there was an abrupt change in the hydrous diffusivity slope around the water content at the fiber saturation point, which could slow down the process of numerical resolution in the hygroscopic field.

Keywords: diffusivity, wood, drying, shrinkage, moisture content, desorption isotherm, *Pinus halepensis* Mill.

Nomenclature

Latin Letters

a_w	Water activity (%)	M_v	Molar mass of water (k g. mol ⁻¹)
c	Concentration (kg.m ⁻³)	P	Pressure (Pa)
D	Moisture diffusivity (m ² .s ⁻¹)	Pr	Prandtl number
D_0	Arrhenius factor (m ² /s)	Re	Reynolds number
d.b	Dry basis	R	Gas constant (8,314 J.mol ⁻¹ k ⁻¹)
e	Thickness of the sample (m)	R_v	Volumetric shrinkage coefficient (%)
F	Mass flow (kg.m ⁻² .s ⁻¹)	t	Time (s)
h	Convective heat transfer coefficient (W.m ⁻² .k ⁻¹)	T	Temperature (°C, K)
k	Mass transfer coefficient (m.s ⁻¹)	U	Speed (m. s ⁻¹)
L	Length of the sample (m)	V	Volume (m ³)
l	Width of the sample (m)	Z	Cartesian coordinate (m)
m	Mass (kg)	X	Moisture content (kg/kg d.b)

Greek letters

ΔH_{vap} Latent heat of water vaporization (J/kg)

ν_{air} Cinematic viscosity of air (m²/s)

β Coefficient of shrinkage

λ_{air} Thermal conductivity of air (W/m)

ρ_s Density of dry solid (kg.m⁻³)

ρ Total mass density (kg.m⁻³)

Subscripts

0 Initial

a Air

cal Calculated

cr Critical

eq Equilibrium

h Humidity

exp Experimental

l Liquid

s Solid

v Vapor

1. Introduction

Material transfer in porous media during drying can be approached both from a theoretical point of view using a formula based essentially on Fick's law [1,2], and from an experimental point of view by measuring the loss of mass during drying. The mechanism of moisture migration inside cellular walls is a problem often discussed. Many authors have linked this mechanism to a simple diffusion of Fick where the potential for transfer would be the water content. Stamm [3] showed that, under these conditions, the activation energy of the process was slightly inferior to the enthalpy necessary to vaporize water, i.e. the sum of the differential heat of sorption and the latent heat of vaporization. To move moisture within the area of interstitial water during conventional convective drying with atmospheric pressure, and a temperature well below the boiling point of water, the essential mechanism for migration is capillarity. However, in cases of convective drying at high temperature [4], external pressure can be lowered outside a solid as a gradient of total pressure in the gas phase which induces a liquid or gas flow able to contribute to the total transfer [5]. Various experimental techniques and numerical methods have been used by several authors [6,7,8,9] to determine the diffusion coefficient of bound water in the wood. However, systematically determining this parameter for each direction of anisotropy in several wood species has not been found yet. Among the methods generally used, significant differences can clearly be seen [10]. In addition, in most studies, the coupling which always exists between mass transfer and heat transfer has definitely been ignored. This is particularly serious when the mass transfer coefficient is ignored at the interface from experimental curves starting from a model with only one variable [11].

Determining the mass diffusion coefficient largely depends on the physical and mechanical properties of the dried product [12]. In the hygroscopic field, bound water diffusion through the wood is assumed to obey Fick's law [13]. This hypothesis agrees with the work of Wadsö [14]. This author showed a nonlinear phenomenon in the case of wood, but the moisture content was higher than that used in this work. The objective of this work is to define the moisture diffusion coefficient of Aleppo pine. The diffusion model, with simplifying assumptions, takes into account the shrinkage of the material during drying [15,16]. The anisotropic hygroscopic properties of the wood and its anatomy affect the transfer phenomena and the drying process becomes more complex. The moisture diffusion coefficient was adjusted to minimize the difference between the experimental water content and the simulated one. The model performances were evaluated following the agreement between the experimental and simulated results.

2. Materials and methods

The drying experiments were performed in a closed loop dryer using forced convection of hot air (Figure 1). The lab dryer consisted of a centrifugal fan with variable speed, a box containing 18 kW batteries for heating,

and a perforated tray connected to the fan by a divergent barrier to prevent flow rotation. Air flow in the perforated tray was perpendicular to the surface of the sample to be dried, in order to provide optimum conditions for contact. An electronic balance located on the lower part of the perforated tray made it possible to measure loss of product mass. Temperature, relative humidity and air velocity inside the perforated tray were controlled and adjusted by an automatic regulating system.

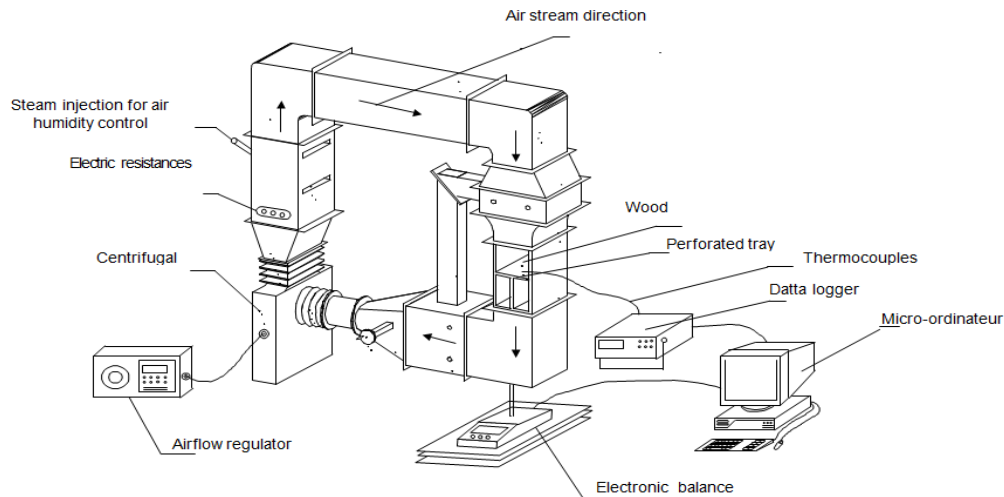


Figure 1: Overall layout of the experimental laboratory dryer.

The samples studied were 30x5x2 cm boards of Aleppo pine wood.

The boards were chosen primarily for their appearance: absence of machining defects (saw marks), knots, curves of the rings, wire, rings, regularity, and absence of compression wood. They were placed on a perforated grid of a perforated tray. The air drying conditions were held constant throughout each test. The weight loss as a function of time was continuously measured on the unit product-plate support using a high-precision balance connected to a data acquisition and processing system. In order to determine oven dry weight, the sample was placed in an oven at 103, 5°C until constant weight. To evaluate the thermal heat gradient within the sample, thermocouples were placed at different points in the sample. The shrinkage was also studied during drying stages. Aleppo Pine wood used for the experiments was grown in the north west of Tunisia. To limit the variability of wood for the drying data all samples are selected from a freshly felled green tree. The boards dimensions were 30 x 5 x 2 cm³ (L x R x T).

3. Diffusive Model

3.1. Mathematical models

The approach consists of numerically solving the equations of the solid and liquid phase continuity. The two equations are coupled by a convective term making the shrinkage speed of the solid phase and the volumetric shrinkage coefficient appear. The formula of this diffusive model is based on the following assumptions:

- The transfer of the water within the product is unidirectional.
- The product is biphasic water-solid.
- Evaporation occurs on the surface.

The continuity equations of the solid and liquid phase are respectively:

$$\frac{\partial C_s}{\partial t} = -\text{div}(C_s \vec{U}_s) \quad (1)$$

$$\frac{\partial C_l}{\partial t} = -\text{div}(C_l \vec{U}_l) \quad (2)$$

The flux liquid density is the amount of diffusive and convective flux due to product shrinkage [17].

$$C_l \vec{U}_l = -\rho D \text{grad} \left(\frac{C_l}{\rho} \right) + C_l \vec{U}^* \quad (3)$$

\vec{U}^* : is the average mass velocity of constituents and confirms the following relation in the case of ideal shrinkage:

$$\vec{U}^* = \frac{C_s \vec{U}_s + C_l \vec{U}_l}{\rho} \quad (4)$$

With:

$$\rho = C_l + C_s$$

$$C_l = C_s \cdot X C$$

$$C_s = \frac{\rho_s}{1 + \beta X}$$

The equation (3) becomes:

$$C_l \vec{U}_l = -C_s \cdot D \overrightarrow{\text{grad}} \left(\frac{C_l}{C_s} \right) + C_l \vec{U}_s = -C_s \cdot D \overrightarrow{\text{grad}}(X) + C_s X \vec{U}_s \quad (5)$$

Thus, the mass conservation equation is

$$\frac{\partial(C_s X)}{\partial t} = \text{div} \left(C_s \cdot D \overrightarrow{\text{grad}}(X) - C_s \vec{U}_s \right) \quad (6)$$

Finally, the liquid and solid phase transfer equations are as follows:

$$\text{Solid:} \quad \frac{\beta}{1 + \beta X} \frac{\partial X}{\partial t} = \frac{\partial U_s}{\partial z} - \frac{U_s \beta}{1 + \beta X} \frac{\partial X}{\partial z} \quad (7)$$

$$\text{Liquid:} \quad \frac{\beta}{1 + \beta X} \frac{\partial X}{\partial t} = \frac{\partial}{\partial z} \left(\frac{D}{1 + \beta X} \frac{\partial X}{\partial z} \right) - \frac{U_s}{1 + \beta X} \frac{\partial X}{\partial z} \quad (8)$$

Initial conditions:

$$t = 0; X = X_0, T = T_0, U_s = 0 \quad (9)$$

Boundary conditions:

$$t > 0; z = 0, \frac{\partial X}{\partial z} = 0, \frac{\partial T}{\partial z} = 0, U_s = 0 \quad (10)$$

$$z = e(t), \frac{\rho_s}{1 + \beta X} \left(-D \frac{\partial X}{\partial z} + X U_s \right) \Big|_e = k_m [a_w(X, T) P_{vsat}(T) - H_r P_{vsat}(T_a + 273, 15)]$$

Mass transfer coefficient, K_m can be determined from the following relationships [18] for laminar flow and turbulent flow, respectively;

$$Sh = \frac{k_m L}{D_0} = 0.332 \text{Re}^{0.5} Sc^{0.33} \quad (11)$$

$$Sh = \frac{k_m L}{D_0} = 0.0296 \text{Re}^{0.8} Sc^{0.33} \quad (12)$$

The heat transfer coefficient, h , is determined by the nature of the air flow in the vicinity of the exchange surface [19].

$$h = 0,232 \frac{\lambda}{L} (\text{Re})^{0.5} \text{Pr}^{0,335} \quad (13)$$

The thermal air conditions applied to the wood slab placed in the dryer are shown in Figure 2.

As the wood shrinks due to water loss, its instantaneous thickness depends on the internal distribution of the water content and can be calculated from the value of the volumetric shrinkage coefficient which should be measured experimentally.

$$e = e_{dry} (1 + \beta X) \quad (14)$$

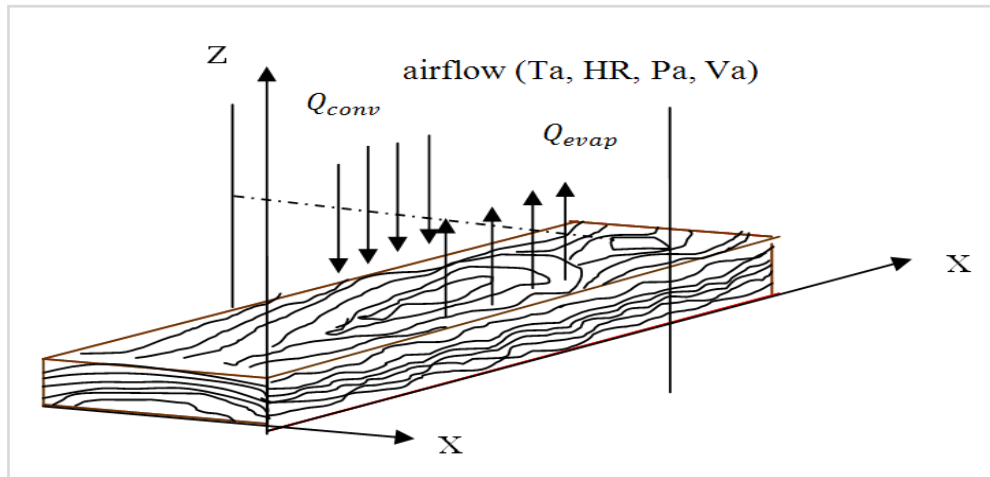


Figure 2: Schematic of the wood slab.

3.2. Numerical simulations

Moisture diffusivity can be determined by minimizing the difference in the experimental values of the water content, in the hygroscopic field and those simulated by the model. The simulation was done using the initial experimental water content value as an initial value of the diffusion coefficient D_0 a value estimated by the literature.

If $(X_{1,cal} - (X_{1,cal} - X_{1,exp}) / X_{1,cal} < \varepsilon$ with $(\varepsilon = 5\%)$, the program recorded the result. Otherwise, the program considered a new value for the diffusion coefficient (test increment). The same procedure was repeated until the stopping criterion was reached. This final value of diffusivity obtained was used to calculate $(X_{2,cal})$. The procedure was reproduced identically for all simulations, until the simulated water content equaled the water content equilibrium of the Aleppo pine wood.

The program used to solve this model made it possible to determine the evolution of the simulated water content during drying and the variation of the coefficient diffusion as a function of the moisture content.

$$\text{We have: } X_e^n = \frac{X_E^n + X_P^n}{2} \text{ and } X_w^n = \frac{X_W^n + X_P^n}{2}; \left. \frac{\partial X}{\partial Z} \right|_e = \frac{X_E - X_P}{\Delta z} \text{ and } \left. \frac{\partial X}{\partial Z} \right|_w = \frac{X_P - X_W}{\Delta z} \quad (15)$$

By performing a one-dimensional spatial and temporal discretization of equation (8), on a control volume where the mesh is assumed to be uniform (Figure 3), the thickness of the board is then subdivided into N fixed elements with thickness Δz and time Δt . The representative coordinates (z,t) of any point are (K,N) , where K and N are two entities belonging to $[0,n]$ and $[0,nt]$, respectively.

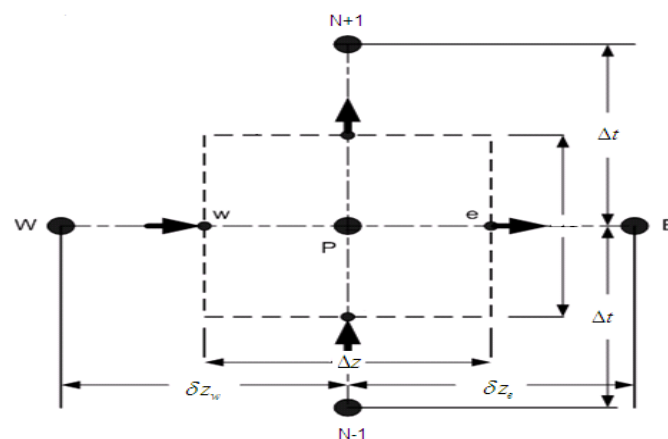


Figure 3: Finite volume discretization.

4. Results and discussion

4.1. Desorption isotherm

The isotherm shows the relationship between the equilibrium moisture content X_{eq} of the studied material and the relative humidity of the environment. A wet product is maintained at a constant temperature and placed in an enclosure where the vacuum is controlled; the pressure variation can then be followed as it increases from a very low value to an equilibrium value due to the contained water evaporating from the product. Thus, the relation between the relative humidity of the product and the corresponding vapor tension of equilibrium constitutes the desorption isotherm [20].

The desorption isotherm is an essential step in the study of drying since it gives valuable information about the hygroscopic equilibrium of the product to dry. To model the desorption curves, many empirical correlations exist in the scientific literature. Among the most adaptable models is that which presents a low quadratic average Error (EQM).

$$EQM = \frac{1}{N} \sum_{i=1}^N |X_{cal} - X_{exp}| \quad (16)$$

Dent's model presents a low EQM compared to other tested models. Its formula is given hereafter:

$$X_{eq} = \frac{HR}{a + HR^2 + b * HR + c} \quad (17)$$

The residual variances are weak of the coefficients corresponding to variations in moisture content of 0,01 and 0,02 kg water kg⁻¹. db (Table 1). This shows the good precision with which Dent's model describes the isothermal curves obtained experimentally [21].

Table 1: Values of the coefficients of eq.14 and residual variances obtained between the evolutions in water content equilibrium calculated with DENT's model and measured during the experiment.

Temperature (°C)	a (-)	b (-)	c (-)	Residual variance
60	-6,9672925	7,9979351	0,7269553	0,01232622
70	-8,1768906	9,3651071	0,68019558	0,01085664
80	-8,3831765	8,7920217	1,5072059	0,01074646

4.2. Kinetics drying

In this experiment, the speed of the air was set at 3 m/s and the relative humidity of the air at 30% for all tests. Only the temperature varied from one test to another. The system was allowed to come to a point of stabilization. The sample was placed on a perforated tray. The weight loss of the ample was measured every 5 minutes.. This procedure led to considerable fluctuations in weight due to the effect of air flow. Some works stopped the air flow and starts the weight loss measurement [22]. Within these conditions the hygroscopic equilibrium of Aleppo pine sample was studied. The relationship between the equilibrium moisture content and the relative humidity is shown in figure4 at different temperature.

The moisture content is given by:

$$X = \frac{m_h - m_{dry}}{m_{dry}} \quad (18)$$

It can clearly be seen that temperature has a great influence on drying time. An increase in temperature causes a rising rate of water evaporation from the center towards the product surface [23].

4.3. Volumetric shrinkage

The total volumetric shrinkage (%) is the difference between the volume of the saturated sample in the water and its oven dried volume. Details of the technique are given by the American Society for Testing and Materials (ASTM) Standard D-143-94 [24]. The phenomenon of shrinkage occurs as soon as the wood humidity becomes lower than the fiber saturation point. Below the fiber saturation point, the wood has the ability to change dimensions which can be expressed differentially along the three principal directions of the wood: (longitudinal, tangential and radial)s. Kumar *et al.* [25] noted that measuring axial shrinkage is extremely delicate (about 0.1 % to 0.3 %) because of the weak water content in the wood. The volumetric shrinkage

measurements showed that the total dimensional variations of 3 samples of wood measuring 2.5 x 10 x 2.5 cm³ RTL had the same variations.

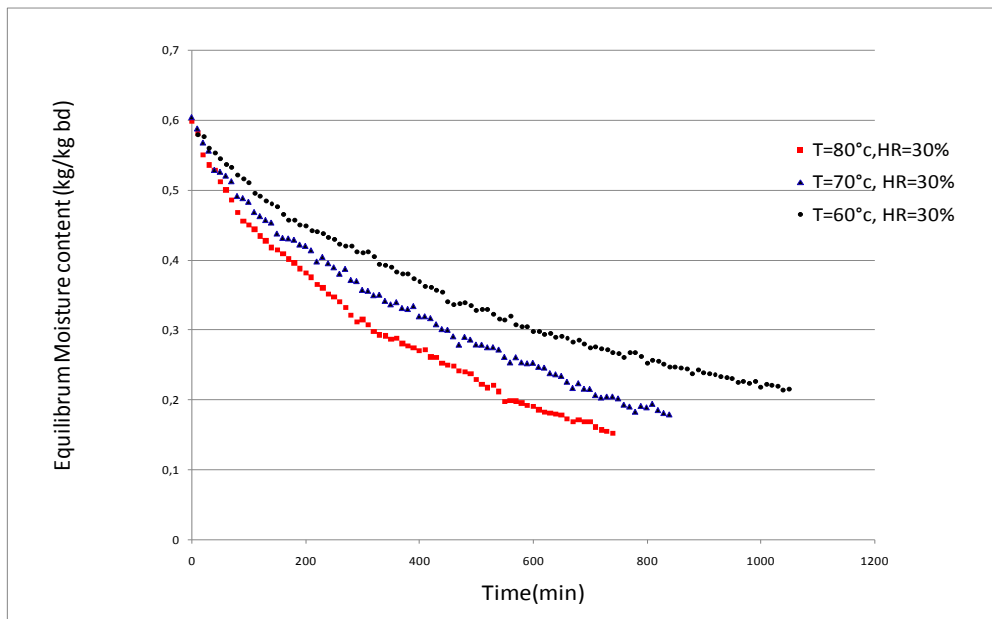


Figure 4: The effect of air temperature on the drying curve of Aleppo pine.

The total shrinkage measurements showed negligible values in the longitudinal direction and then neglected in this study.

The volumetric measurement of shrinkage gave a fiber saturation point value of about 0,30. Thus, this value plays a significant role in the diffusive model. In the hygroscopic range, the evolution of shrinkage in relation to moisture content is linear (Figure 5); above the fiber saturation point, the volumetric shrinkage is constant. The value of maximum shrinkage can therefore be deduced, $R_{v_{max}}=16\%$, for $a_w = X_{fib} = 0.30$ for

$$R_v(\%) = (V_h - V_{dry}) / V_{dry} \quad (17)$$

However, volumetric shrinkage has a significant standard deviation of about 2,78. If compared to the value found by Charron et al. [26] for larch wood, it would have a total volumetric shrinkage of 15.16% and a standard deviation of 2.88. Heurtematte *et al.* [27] qualified wood according to coefficient values of volumetric shrinkage which is the volume variation between the anhydrous state and the air saturation state.

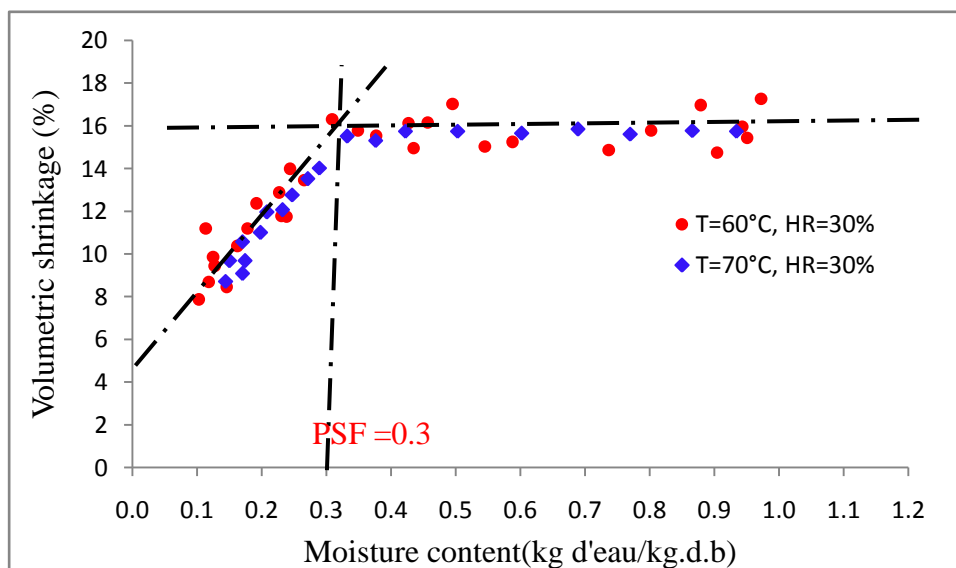


Figure 5: Evolution of volumetric shrinkage as a function of relative humidity.

4.4. Validation of the numerical results

The equations with the corresponding boundary conditions are solved on a deformable mesh, while keeping a fixed number of nodes and by adjusting spacing over time. Indeed, with each new step of time, the mesh sizes are adapted starting from the shrinkage equation, expressing the thickness of wood according to average moisture content of the preceding step. The discretization of the transfer equation of the liquid phase (Equation 8) was carried out by the method of finished volumes [28], and the equation of transfer of the solid phase (Equation 7) was performed by Rung-Kutta's method the 4th order. The model was fit with FORTRAN 4, 0. Figures 6, 7 and 8 show a good agreement between the simulated and the experimental values of the moisture content. The minimization, applied in the model, identifies the diffusion coefficient. The evolutions of the moisture content, envisaged by the experimental measurement, are adjusted in the diffusive model in a form of a correlation for the simulation.

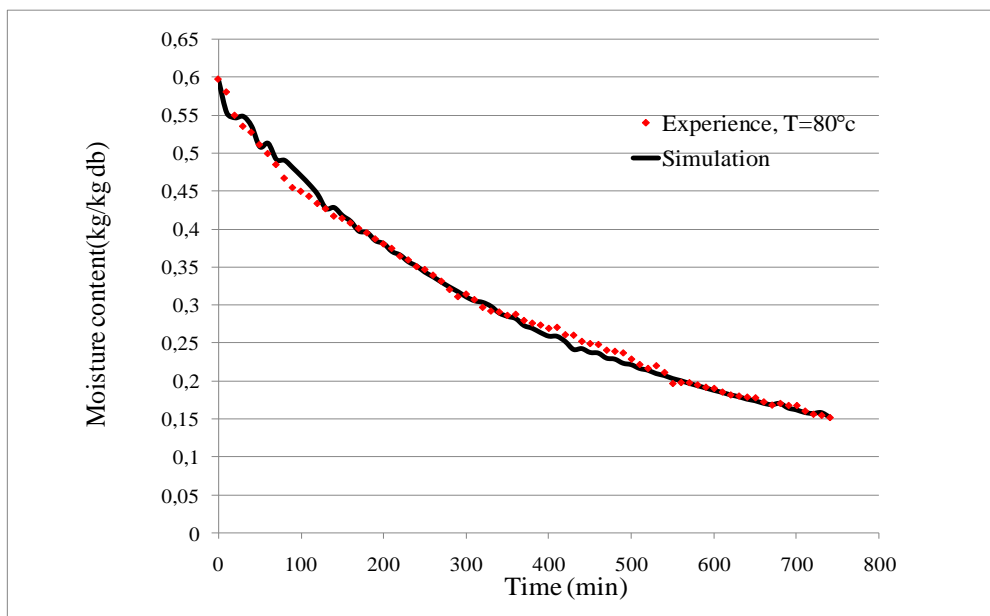


Figure 6: Temporal evolution of the water content.

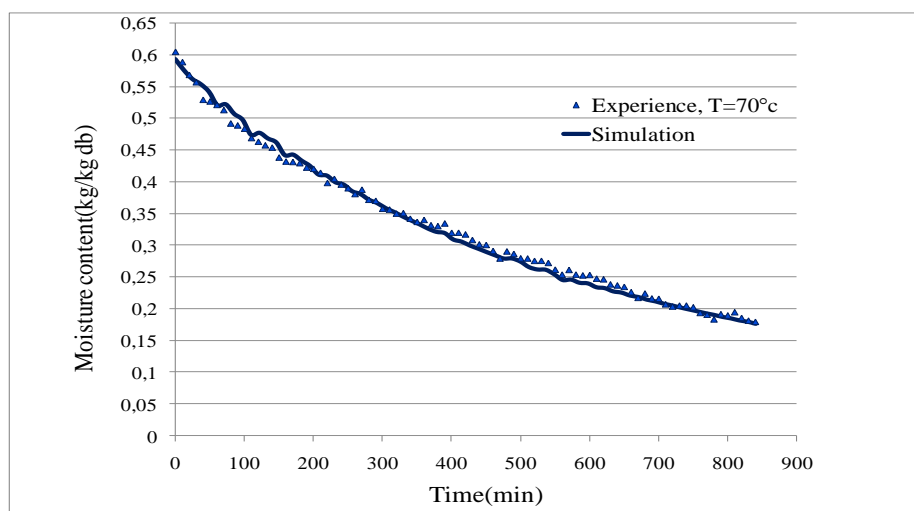


Figure 7: Temporal evolution of the water content.

4.5. Moisture diffusion

Mass transfer can include two basic phenomena, the external convection represented by the mass transfer coefficient and the diffusion represented by the diffusion coefficient, responsible for the water transport under the effect of a gradient of water content. Figure 9 represents the variation in the diffusion coefficient, identified

by the diffusive model (taking into account the velocity of the shrinkage) in function of the water content during drying. The fiber saturation point separates between two fields: the free water in the lumen and is subjected to capillary forces and gravity. The basic mechanism for the migration of the bound water molecule is the capillary affecting physical and mechanical properties of the wood. Siau [2] improved the concept using the concentration gradient of activated molecules. In this case, Fick's law would remain valid because the diffusion takes place only after the activation of water molecules. The diffusion coefficient is often a function of the temperature and the moisture content.

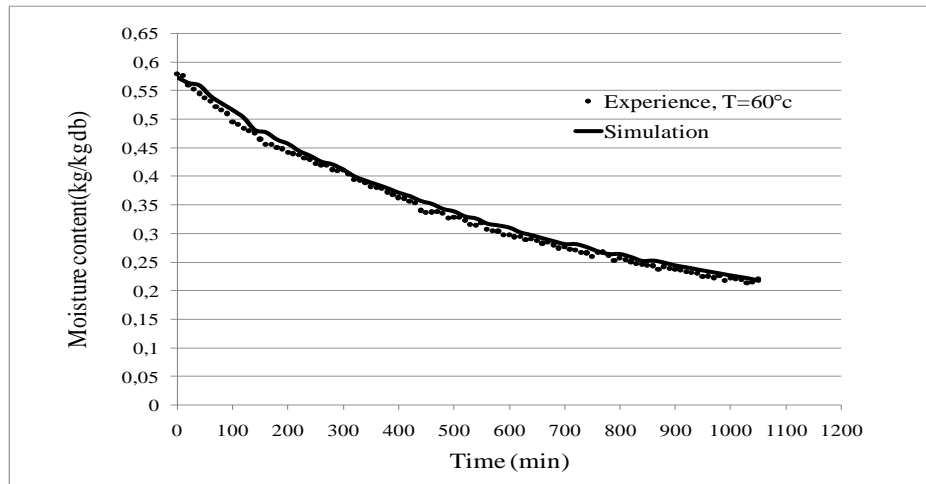


Figure 8: Temporal evolution of the water content.

At a constant relative humidity the increase of the air temperature the moisture diffusion speeds up (Figure 9) while the diffusion coefficient decreases during drying, air flow varying between $1.7 \cdot 10^{-11} \text{ m}^2 \cdot \text{s}^{-1}$ and $3.4 \cdot 10^{-11} \text{ m}^2 \cdot \text{s}^{-1}$ which is in agreement with the values published in the literature. Lartigue [29] gave values of D for Maritime pine between $0.12 \cdot 10^{-09} \text{ m}^2 \cdot \text{s}^{-1}$ and $0.3 \cdot 10^{-09} \text{ m}^2 \cdot \text{s}^{-1}$ depending on the temperature.

Water properties are strongly dependent on moisture content and temperature. Moreover, an increase in temperature, according to the Arrhenius law expression, generally results in an increase in the velocity of the diffusion. A correlation with moisture content was carried out. The evolution is almost quasi-exponential; we are limited to a simple correlation:

This model was tested for different temperatures. It is relatively good for the entire range of moisture of the hygroscopic field and it is best appropriate for the moisture content of 0.35 (fiber saturation point of 0.15, in the vicinity of moisture content of equilibrium). Other models were tested. The correlations are not good for a humidity higher than 0.15.

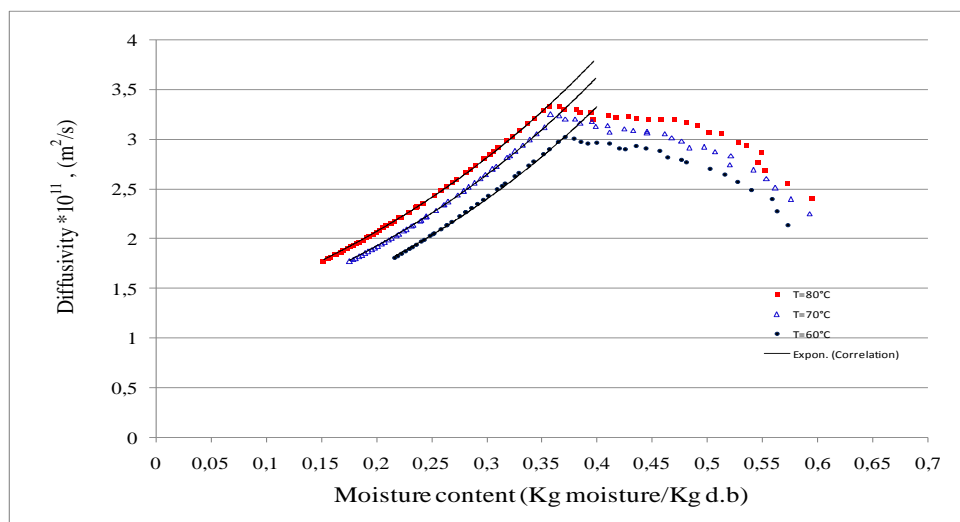


Figure 9: Variation of the moisture diffusion coefficient

The mass diffusion coefficient is described by different mathematical relationships. The influence of the moisture content is represented by a polynomial law or an exponential law [29]. In this case, the expression of the mass diffusivity of water can be written in the following form:

$$D(X, T) = D_0 \exp\left(-\frac{E_a}{RT}\right) \exp(-(AT + B)X) \quad (18)$$

The expression of the coefficient of water diffusion in Aleppo pine wood is as follows:

$$D(X, T) = 3,9 \times 10^{-11} \times \exp\left(-\frac{137,031}{RT}\right) \times \exp\left((3,5 \times 10^{-3} \times T - 2,363)X\right) \quad (19)$$

The moisture diffusion coefficient equation in this case makes it possible for us to estimate the value of the activation energy of the water diffusion in the hygroscopic $E_a = 137.031$ kJ/ mol. This value is plausible if we compare it with the values of the activation energy found by Ricardo *et al.* [30] which are represented in Table 2.

Table 2. Values of Aleppo pine wood activation energy (this work) and other types of wood (Ricardo [30]).

Wood	Aleppo pine (present work)	Loblolly pine	Sweetgum	Red Oak	Eucalyptus nitens
Ea(kJ/mol)	137,031	135	131	135	139

Conclusion

A one-dimensional diffusive model was developed to simulate the moisture behavior of water in wood during drying using the finite-volume method. This model is based on simplifying assumptions relating not only to the geometry of the part studied but also to its behavior; in order to guarantee the relevance of the results, the validity of each assumption must be carefully examined.

Thermophysical coefficients inserted in our equations were those obtained with our wood and presented in the literature. On the experimental level, we determined the drying kinetics, the desorption isotherm and the volumetric shrinkage. The numerical simulation allowed us to identify the diffusion coefficient of the Aleppo pine in the decreasing speed phase of drying. The moisture content of the fiber saturation point was considered a critical value in the diffusive model. It should be noted, nevertheless, that there is still a slight difference between the experimental points and the results of the numerical simulation. This difference was the consequence of the simplifying assumptions adopted, and some thermophysical coefficients obtained from the wood should be included, other than those of studies and errors recorded during the experiments, thus making it possible to obtain the experimental kinetics, the desorption isotherms and the volumetric shrinkage. A predictive correlation of diffusivity as a function of temperature and moisture content was determined for Aleppo pine wood.

Bibliography

1. Agoua E., Zohoun S., Perre P. *Inter. J. Heat Mass Transfer* 44 (2001) 3731-3744.
2. Siau J.F. Department of Wood Science and Forest Products., Virginia Polytechnic Institute and State University., Blacksburg, USA, (1995).
3. Stamm A.J. *Wood Sci. Technol* 1 (1967) 122-141.
4. Moyne C., Martin M. *Inter. J. Heat Mass Transfer* 25 (1982) 839-1848.
5. Moyne C. *Advances Water Resources* 20 (1997) 63-76.
6. Tagne M.S., Zoulalian A., Njomo D., Bonoma B. *Revue des Energies Renouvelables* 14 (2011) 487-500.
7. Nasrallah S.B., Perre P. *Inter. J. Heat Mass Transfer* 31(1988) 957-967.
8. Rosen H.N. *Wood Fiber sci.* 10 (1978) 218-228.
9. Comstock G.L. *Forest Products J.* (1963) 97-103.
10. Chen Y., Choong E.T., Weizel D.M. *Wood Fiber Sci.* 27 (1995) 178-182.
11. Chen Y., Choong, E.T., Weizel D.M., *Wood Fiber Sci.* 28 (1996) 338-345.
12. Simpson W.T., *Wood Sci.Technol.* 27 (2005) 409-420.

13. De Meijer M., Avn Der Zwan P.P., Militz H. *Holzforschung – Inter. J. Biology, Chemistry, Physics Tech. Wood* 50 (1996) 135-142.
14. Wadsö L., *Wood Fiber Science* 26 (1994) 36-50.
15. Hassini L., Azzouz S., Peczalski R., Belghith A., *J. Food Engineering* 39 (2007) 47-56.
16. Azzouz S., Guizani A., Jomaa W., Belghith, A., *J. Food Engineering* 55 (2002) 323-330.
17. Bird R.B., Stewart W.E., Lightfoot E.N. *Transport phenomena*, second ed., John Wiley and Sons., USA, (2002).
18. Mills A.F. *Basic heat and mass transfer*, Massachusetts: Irwin, (1999).
19. Incropera F.D., Dewitt D.P. *Fundamentals of Heat and Mass Transfer.*, seventh ed., John Wiley and Sons., USA, (2011).
20. Belghit A., Kouhila M., Boutaleb B.C., *Rev. Energ. Ren.* 2 (1999) 87-97.
21. Janas S., Malumba P., Deroanne C., Béra F., *Biotechnol. Agron. Soc. Environ* 14 (2010) 389-398.
22. Ferrao P., Figueiredo A., Freire F., *Drying Technology: Inter .J.* 16 (1998) 1687-1702.
23. Perre P., Degiovanni A., *Inter. J. Heat Mass Transfer* 33 (1989) 2463-2478.
24. ASTM D-143-94. *Standard Test Methods for Small Clear Specimens of Timber*, American Society for Testing and Materials, USA, (2000).
25. Kumar R.R., Kolar A.K., Leckner B., *Biomass Bioenergy* 30 (2006) 153-165.
26. Charron S., Jourez B., Marchal M., Hébert J., *Biotechnol. Agron. Soc. Environ* 7 (2003) 5-16.
27. Heurtematte J., Orus M., Pouzeau P., Le Sage R. *Usinage du Bois.*, Paris, France, (1985).
28. Patankar S.V. *Numerical Heat Transfer and Fluid Flow*; Hemisphere Publishing, New York, (1980).
29. Lartigue C. *Les Mécanismes Elémentaires mis en jeu lors du Séchage du Pin Maritime.*, Thèse de doctorat, Université de Bordeaux, (1987).
30. Ricardo B.S., Ewelyn A.C., Mikhail Y.B., Hou-Min Hasan C.J., *BioResources* 6 (2011) 3623-3637.

(2016) ; <http://www.jmaterenvirosci.com/>